ASSESSMENT AND PREDICTION OF THE THERMAL PERFORMANCE OF A CENTRALIZED LATENT HEAT THERMAL ENERGY STORAGE UTILIZING ARTIFICIAL NEURAL NETWORK

Azeldin El-Sawi	Fariborz Haghighat	Hashem Akbari
Ph.D. Candidate	Professor Concordia Research Chair - Energy & Environment	Professor

Department of Building, Civil and Environmental Engineering
Concordia University,
Montréal, Québec H3G 1M8, Canada

ABSTRACT

A simulation tool is developed to analyze the thermal performance of a centralized latent heat thermal energy storage system (LHTES) using computational fluid dynamics (CFD). The LHTES system is integrated with a mechanical ventilation system. Paraffin RT20 was used as a phase change material (PCM) and fins are used to enhance its performance. Due to the fact that the numerical calculations take a longer time, the simulations are performed on the first day of each week through summer months and then the database is used to train an artificial neural network (ANN) for predicting of the performance. Then, the LHTES's outlet air-temperature function is integrated into the TRNSYS building thermal response model. The trained ANN is able to improve the prediction of the LHTES's outlet air-temperature for a wide range of inlet conditions (i.e., air-temperature and flow rate). We found that the indoor air-temperature is reduced by about 1.5-2.5℃.

1. INTRODUCTION

Conventional cooling systems require a considerable amount of primary energy resulting in an increase of building operation cost. As a result, the greenhouse gas (GHG) emissions are accordingly boosting. (Parameshwaran, Kalaiselvam et al. 2012) reported that the building sector in developed nations uses about 40% of the world-wide total energy and contribute up-to 40% of GHG. Thus, the need to searching for new alternative source of energy becomes desperately crucial. Thermal energy storage (TES) systems are considered as the best option to shift the electrical energy demand from on-peak hours to off-peak hours during the day-time. Among different technologies of TES, latent heat thermal energy storage (LHTES) systems are employed to serve as a tool for storing the coolness from the ambient inlet air in PCM medium to be used for stabilizing the fluctuation of indoor air temperature during the day-time. Thus, the thermal comfort conditions have been improved.

LHTES is a promising technology for building heating and cooling applications. A centralized LHTES system is a hybrid phase change material (PCM) closed system based multi-fin heat sink. PCMs are used as a heat transfer medium in LHTES systems to store and release energy. PCMs can be divided into three subcategories based on phase change state: solid-liquid, liquid-gas, and solid-gas PCMs. Practically, the solid-liquid PCMs are more likely to be utilized for LHTES systems, (Zhou, Zhao et al. 2012). A variety of PCMs, available with different thermo-physical properties, are used for LHTES systems, which utilize a change in the phase of PCMs. For instance, two types of PCMs that are commonly used are paraffin wax and salt hydrate, which are categorized as organic and inorganic PCMs, respectively.

During the past decade, LHTES systems and their applications have received a wide attention from building researchers and practitioners, due to relatively large heat storage capacities. A centralized LHTES system has a great potential to be integrated into HVAC system for peak load shaving. Generally, the energy storage technologies help to shift on-peak hour energy demand to off-peak hour during the day,(Soares, Costa et al. 2013). Thus, the electricity supplied from a power generation plant is expected to minimize thereby mitigating the greenhouse gases emission. However, (Agyenim, Hewitt et al. 2010) reported that most PCMs have low thermal conductivity. (Dincer, Ermis et al. 2007) applied a feed-forward back-propagation artificial neural networks (ANN) algorithm to analyze heat transfer through annularly finned tube with PCM, concluding that ANN approach is a promising method for analyzing thermal energy storage systems within a maximum discrepancy of about 5% compared to a numerical solution.

(Arkar and Medved 2007) studied the free cooling of a low-energy building using an integrated LHTES system with a mechanical ventilation system where they used spherical encapsulated RT20 paraffin (PCM). A periodic variation of the inlet ambient-air temperature was considered in a developed numerical packed-bed model in order to obtain the optimum phase-change temperature. The distributions of the air axial velocity and the bed porosity were considered uniform and applied into coupled energy equations for the air and PCM. The outlet-air temperature of LHTES system was approximated as Fourier functions and then integrated into the TRNSYS building thermal model. The selected building has a floor area of 191m^2. The simulation results showed that a PCM with a melting temperature between 20 and 22℃ has a significant potential to be implemented for free cooling for continental climate, characterized by hot summers and cold winters. They reported that the LHTES with 6.4kg of PCM per m^2 of floor area can afford suitable thermal comfort conditions inside the selected building.

The centralized LHTES system is integrated into a mechanical ventilation system through suitable air supply ducts inside a room of the building to store/retrieve the thermal energy, which leads to justify the indoor air temperature variation during the day-time, as shown in Figure 1. To regulate the function of a mechanical ventilation system, a control unit is required to balance the temperature difference between the inlet ambient air, T_a and outlet air from LHTES system, T_{out}. Thus, the ventilation system has two modes of operation. First mode is to restrict the air flow to just pass through the LHTES system as the ambient air temperature is higher than the set point temperature as shown in Figure 1 (a). Second mode is to allow ambient air directly supplied to the room and also to pass through the LHTES system thereby storing cold energy when the ambient air temperature is lower than the set point temperature as shown in Figure 1 (b).

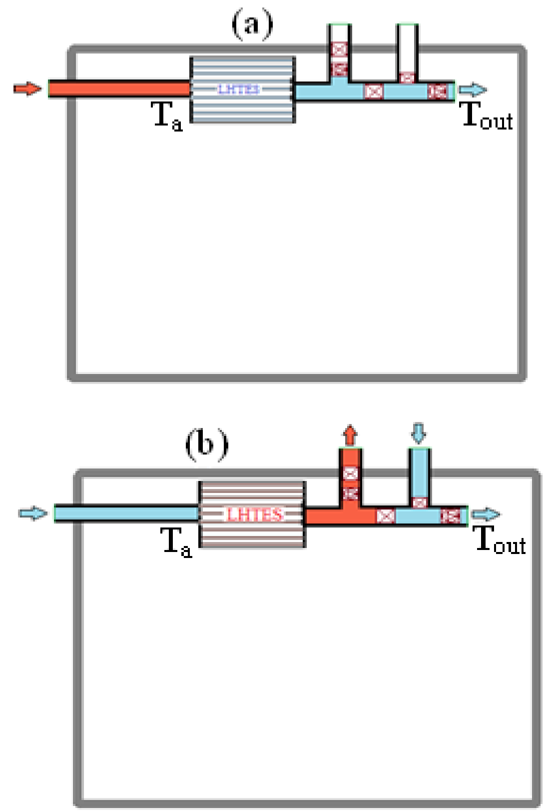

Figure 1. Installation of The Centralized Latent Heat Thermal Energy Storage System (LHTES) in Two Ventilation Control Modes; (A) Discharging Mode, (B) Charging Mode

In this study, we implemented a validated three-dimensional mathematical model of the centralized LHTES system for analyzing the thermal performance of melting and solidification processes for both quasi-steady state and transient conjugate heat transfer problem. An extensive CFD simulation is carried out to study the long-term performance of a centralized LHTES. A validate CFD simulation tool is integrated with a building mechanical ventilation system. Paraffin RT20 is used as a PCM and fins are used to enhance its performance. ANN is developed to predict the LHTES's outlet air-temperature. Then, the trained ANN function is integrated into TRNSYS building model to study the performance of a LHTES for application in Montreal.

2. PHYSICAL MODEL AND DESCRIPTION

In an earlier study, we documented the development and validation of a CFD model to characterize the performance of PCM (A. El-Sawi, F. Haghighat et al. 2013). Fig. 2 shows the schematic diagram of the three-dimensional computational domain storage unit filled with PCMs where the aluminum fins are arranged orthogonal to the axis of the unit. The heat transfer fluid flows in the vicinity of such unit. The model has three zones; 1) Air box with airflow around the fins and system, 2) PCM box (fluid/solid), and 3) Fins box (solid). The fins on the external side of the box are to increase the exposed area for convective heat flux whilst fins inside the box are aimed at boosting the thermal conduction heat flux. The box is filled with paraffin, RT20, with a phase change range of 22-25°C, mass of 3.6kg, heat storage capacity of 172 kJ kg^{-1} within an operating temperature range of 11-26°C and specific heat capacity of 1.8 and 2.4 kJ kg^{-1} K^{-1} for solid and liquid, respectively. For more details about the experimental model, see (Stritih and Butala 2010). A computational fluid dynamics (CFD) package, Fluent, 12 (ANSYS FLUENT 12.0 User's Guide), is used to solve the governing equations for heat flow and phase change problem.

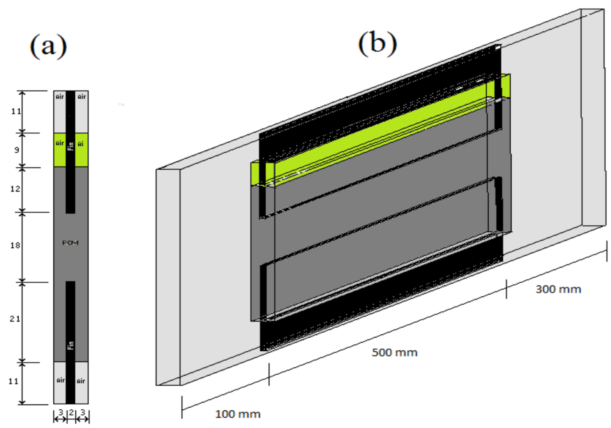

Figure 2. Geometrical Configuration of The LHTES Unit: (a) The Schematic Figure of LHTES System, Cross Section of Computational Domain in Two-Dimensional; (b) Three-Dimensional of Computational Domain.

Numerical technique is employed to simulate PCM heat transfer within a range of a certain temperature, which typically used the enthalpy porosity theory to deal with solid-liquid interface. The porosity effect found to be similar to the liquid volume fraction of the porous media at mushy regions (Brent, Voller et al. 1988). In point of view multiphase flow model such as volume of fluid method (VOF), mixture and Euler model, only VOF and solidification/melting model can be applied simultaneously. (Voller and Swaminathan 1991) developed a method in order to track the solid-liquid interface positions. The method updates the liquid friction at each unit cell at each time step in the entire computational domain.

For seeking simplicity, the following assumptions are considered:

- The axial conduction and viscous dissipation in the fluid are negligible.
- PCM and porous matrix material are considered homogenous and isotropic.
- The thermo-physical properties of the PCM and transfer fluid are independent of temperature. However, the properties of the PCM could be different in the solid and liquid phases.
- The occurrence of the PCM melting is considered at a single temperature T_m.
- The effect of radiation heat transfer is negligible.

2.1 Governing Equations

The governing equations are implemented to describe the fluid flow and heat transfer characteristics of PCM and heat transfer fluid (HTF). The developed model is verified by using available experimental data which can be found in the literature (Stritih and Butala 2010). Density and dynamic viscosity of the liquid PCM depend on its temperature. The density is introduced as follows:

$$\rho = \frac{\rho_l}{\beta(T-T_l)+1} \qquad (1)$$

where $\rho_{(PCM)}$ is the density of PCM; ρ_l is the reference density of PCM at the melting temperature; T_l , and β is the expansion factor. The value of $\beta = 0.001$ has been selected based on the analysis of the detailed data presented by (Humphries and Griggs 1977).

The dynamic viscosity of the liquid PCM has been introduced as (Reid, Prausnitz et al. 1987)

$$\mu = exp\left(A + \frac{B}{T}\right) \qquad (2)$$

where $A = -4.25$ and $B = 1790$ are coefficients.

The energy equation could be written in terms of the sensible enthalpy as following;

$$h = \int_{T_{ref}}^{T} c dT \qquad (3)$$

$$\frac{\partial \rho h}{\partial t} + div(\rho \underline{u} h) = div((k/c)\, grad\, h) + S_h \qquad (4)$$

where k is the thermal conductivity, c is the specific heat, and S_h is the latent heat source term. In order to describe the fluid flow of full liquid and mushy regions, the conservation equations of momentum and mass is crucially required. In the enthalpy-porosity approach, the energy equation source term (S_h) which is accounted for the latent heat evolution could be written in the following form:

$$S_h = \frac{\partial(\rho \Delta H)}{\partial t} + div(\rho \underline{u} \Delta H) \qquad (5)$$

where $\Delta H = F(T)$, the latent heat content, is recognized as a function of temperature.In fact, value of $F(T)$ can be generalized as follows;

$$F(T) = \begin{cases} L, & T \geq T_{liquid} \\ L(1-f_s), & T_{liquid} \geq T \geq T_{solid} \\ 0, & T < T_{solid} \end{cases} \quad (6)$$

where L is the latent heat of phase change. Assuming a Newtonian laminar flow, such equations could be in following forms:

$$\frac{\partial(\rho u)}{\partial t} + div(\rho \underline{u} u) = div(\mu \, grad \, u) - \frac{\partial P}{\partial x} + Au \quad (7)$$

$$\frac{\partial(\rho v)}{\partial t} + div(\rho \underline{u} v) = div(\mu \, grad \, v) - \frac{\partial P}{\partial y} + Av + S_b \quad (8)$$

$$\frac{\partial(\rho w)}{\partial t} + div(\rho \underline{u} \, w) = div(\mu \, grad \, w) - \frac{\partial P}{\partial z} + Aw \quad (9)$$

$$\frac{\partial(\rho)}{\partial t} + div(\rho \underline{u}) = 0 \quad (10)$$

where $\underline{u} = (u, v, w)$ is the velocity, P is the effective pressure, S_b is the buoyancy source term, and μ is the viscosity.

$$S_b = \rho_{ref} g \beta (h - h_{ref})/c \quad (11)$$

where β is the thermal expansion coefficient and h_{ref} and ρ_{ref} are reference values of enthalpy and density respectively (Brent, Voller et al. 1988).

The total enthalpy of the material can be introduced as

$$H = h + \Delta H \quad (12)$$

where

$$h = h_{ref} + \int_{T_{ref}}^{T} c \, dT \quad (13)$$

and h_{ref} is the reference enthalpy, T_{ref} is the reference temperature, and c is the specific heat at constant pressure. The total enthalpy, H, is the sum of sensible heat, $h = cT$, and latent heat ΔH.

The liquid friction, f can be expressed as;

$$f = \begin{cases} 0 & T < T_{solid} \\ 1 & T > T_{liquid} \\ \dfrac{(T - T_{solid})}{(T_{liquid} - T_{solid})} & T_{solid} < T < T_{liquid} \end{cases}$$

In terms of the latent heat of the material, the latent heat content can be written in the following form;

$$\Delta H = fL \quad (14)$$

In the enthalpy-porosity technique, the mushy region (partially solidified region) is treated as a porous medium. For the purpose of the methodology development, it is worthwhile to consider the whole cavity as porous medium. In fully solidified regions, the porosity, λ, is set to be equal zero and takes the values, $\lambda = 1$, in fully liquidus regions, while in mushy regions lies between 0 and 1. Accordingly, the flow velocity is linked to the porosity state and is defined as:

$$u = \lambda u_i \quad (15)$$

where u_i is the real flow velocity.

To describe the flow of a fluid through a porous medium, it is necessary to introduce Darcy's law as:

$$u = -\left(\frac{K}{\mu}\right) gardP \quad (16)$$

where K is the permeability, which is considered as a function of the porosity.

Based on Darcy's law, the Carman-Koseny equation can be written, (Carman 1937) as;

$$gradP = -\frac{C(1-\lambda)^2}{\lambda^3 u} \quad (17)$$

It is suggested that the following formula for the porosity function A can be presented as;

$$A = -\frac{C(1-\lambda)^2}{\lambda^3 + \omega} \quad (18)$$

The value of C is related to morphological properties of the porous medium, and it is assumed constant of 1.6×10^5. The constant ω is used to avoid dividing over zero and is set to be 10^{-3} ·(Voller, Cross et al. 1987).

2.2. Boundary and Initial Conditions

Initial and boundary conditions are referred to experimental setup as (Stritih and Butala 2010). The whole initial computational domain is set to be at the ambient temperature. In addition, the boundary condition in each side of the wall is adiabatic. The symmetry boundary conditions can be applied in a half of a computational domain to reduce the calculation time as shown in Figure.2. The following the initial and boundary conditions are applied to solve the governing equations:

Initial condition

$$t = 0, \quad T = T_i = 288.15\text{K}$$
$$u = v = 0, \quad w = 1.5\text{m/s}$$

Symmetry boundary conditions at side:

$$\left.\frac{dT}{dx}\right|_{x=0} = \left.\frac{dT}{dx}\right|_{x=L} = 0,$$

$$\left.\frac{dT}{dy}\right|_{y=-H/2} = \left.\frac{dT}{dy}\right|_{y=H/2} = \alpha\left(T_{out,i} - T_{in,i}\right)$$

where α is the convection coefficient.

The computational grid is selected based on a grid study for two cases of grid mesh. First case is meshed as follows, bottom fin Domain of 3200, fluid of 204200, PCM of 19800, and top fin of 3200 elements. Second case is chosen, which has been built of 6400 for bottom fin; 6400 for top fin; 78800 for HTF; 39600 elements for PCM. After examining the grid refinement, the time step size is chosen to set as a variable starting from 10^{-5}. The convergence criterion is checked at each time step to 10^{-4} for momentum and 10^{-6} for continuity and energy equations. Properties of paraffin RT20, air, and aluminum used are given in Table.1.

2.3. Model Validation

Figure. 3 presents the comparison between the numerical result and experimental work (Stritih and Butala 2010) for 3-D diagram of completion's air cooling. This graph is obtained from the surface plane for simulation of two cases of the inlet air conditions (i.e., T_i=36, 40°C) with two different scenarios of air flows (i.e., u_i=1.5, 2.4m/s). The numerical model prediction is in a good agreement with the experimental data. The computational result of completion's air cooling time of the LHTES system varies within 2% to 8% for air flow of 1.5m/s.

During the numerical calculations, the variation of PCM's thermo-physical with temperature and also the volume expansion due to the phase change are taken into account by leaving 18% filled up with air above PCM of the total PCM enclosed space. However, a slight deviation is found when the flow rate is of 2.4m/s. The possible reason can be attributed to the length of air channel that is located at over and bottom of the PCM's metal box is not appropriate for flow rate higher than 1.5m/s as (Stritih and Butala 2010) reported in their experimental observations. Therefore, the predicted results can be acceptable as a guide manual to design a practical engineering of LHTES model for cooling applications.

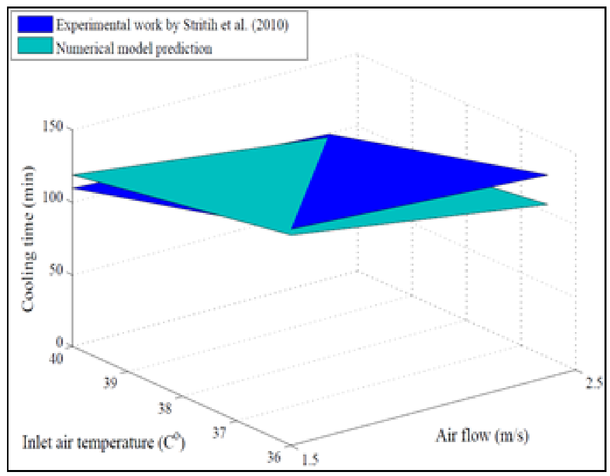

Figure 3. The Comparison of Air Cooling Time Completion Between The Present Numerical Model and The Experimental Work (Stritih and Butala 2010)

Table 1. Properties of Paraffin, Gallium, Air, And Aluminum Used For Calculation

Materials	ρ (kg/m3)	k (W/m K)	c_p (J/kg K)	T_{PCM} (°C)	L (J/kg)	μ (kg/m s)
Paraffin	740/(0.001×(T− 293.15)+1)	0.15	RT20 (DSC)	20-22	172000	0.001×exp (− 4.25+1970/T)
Gallium	6093	32	381.5	29.78	80160	1.81×10-3
Air	1.2×10-5 T 2 − 0.01134T +3.498	0.0242	1006.43	–	–	1.7894×10-5
Aluminum	2719	202.4	871	–	–	–

3. DEVELOPMENT ARTIFICIAL NEURAL NETWORKS (ANN)

The thermal performance of the centralized LHTES system is calculated using computational fluid dynamics (CFD) numerical model. Typically, the required computational time is expensive to completion a simulation for one day due to the complexity of the phase change phenomenon. To predict the thermal performance over a wide range of a year, ANN method is effectively able to extrapolate the LHTES's outlet air-temperature which is calculated by CFD. A generalized GMDH-type (group method of data handling) artificial neural network (ANN) is implemented to provide a predictable thermal performance over a long period of time by training an extensive data obtained from CFD numerical results.

A generalized GMDH-type is implemented to integrate with the obtained numerical results. A generalization of neutral network improved the connectivity configuration to provide an optimal network in which hidden layers and numbers of neurons were more effective to describe the dependent variable of heat transfer phase change process in a polynomial expression. A genetic algorithm is involved in GMDH-type to find effectively the values of quadratic coefficients. This method provides flexibility to manage the neutral networks with different length and size and capability of crossing over the information by changing building blocks. As a result, either small or large number of input variables can be effectively modeled.

The classical GMDH algorithm can be described as a group of neurons where each pairs of neurons is tied using a quadratic polynomial at each layer so that a new generation of neurons will be produced for the next layer. Thus, the output will be a consequence of this reproduction process. Finally, the target is to reach an approximate function value, $\bar{f}$ of output close to the actual one, f for a given input vector, $X = (x_1, x_2, x_3, \dots, x_n)$. Furthermore, the square difference between the actual and predicted functions should be minimized to ensure a reasonable accuracy. Farlow presented a polynomial form to related the input to output (Farlow 1984);

$$y = a_0 + \sum_{i=1}^{n} a_i x_i + \sum_{i,j=1}^{n} a_{ij} x_i x_j + \sum_{i,j,k=1}^{n} a_{ijk} x_i x_j x_k + \cdots \qquad (19)$$

This formula can be simplified for two input variables into the quadratic polynomial form which is most often used to predict the output $\bar{f}$ as following (Ivakhnenko 1971);

$$\bar{f} = G(x_i, x_j) = a_0 + a_1 x_i + a_2 x_j + a_3 x_i x_j + a_4 x_i^2 + a_5 x_j^2 \qquad (20)$$

The evolved two-hidden layers of a typical GMDH-type neural network structure are illustrated in Figure. 4 and the coefficients a_i in Eq. (19) can be determined using regression techniques so that the output $\bar{f}$ is calculated for each pair of x_i, x_j as input variables. A tree of polynomials is built up where the coefficients are determined using the quadratic form in a least-square sense. The general structure of GMDH-type neural network is evolved in which neurons are connected to each other for all layers. Thus, an optimally fit of the output in the entre set of input and output data is achieved for each connected pair of input-output data through quadratic function, G.

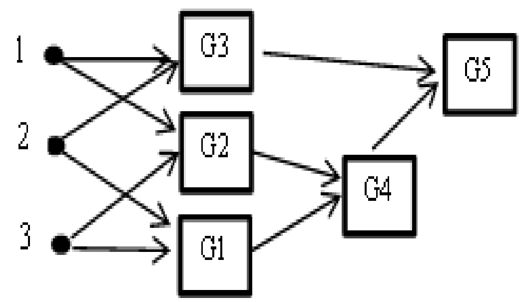

Figure.4 A Typical Feed Forward GMDH-Type Network

4. INTEGRATING THE CENTRALIZED LHTES SYSTEM INTO THE BUILDING

4.1. <u>The Building Model Description</u>

The thermal building response is simulated used TRNSYS for single-zone model. The model is an apartment with dimensions of 11.44m ×5.69m×2.76m. Each wall of the apartment is divided in several layers of materials, which forms a composite wall, more details are provided in Table 2. Floor area is having a dimension of 11.44m×5.69m. Exterior walls, façade (5.69m×2.76m) are facing south-north directions. In the south side, there is one door and one window with surface areas of 1.98, 2.07m^2, respectively and one door, two windows with 2.07, 1.41m^2, respectively in north side. Two adjacent apartments are in vicinity of the considered model on west-east directions.

Table 2. Characteristics of Compositions Material of the Walls of The Typical Building of Montréal (1940-1960)

Composite wall layers	Conductivity [W/m.k]	Capacitance [kJ/kg.K]	Density [kg/m^3]
Heavy wood	0.23	2.40.	650
Light wood (floor)	0.13	1.20	500
Plasterboard BA13	0.32	0.80	790
Plaster coating	0.35	1.00	1500
Solid brick	1.17	0.79	1700
Mineral wool	0.05	0.84	100
Asphalt felt	0.50	1.00	1700
Air (20°C)	-	0.71	1.204

The thermal building response is investigated for free cooling using a mechanical ventilation system with the centralized LHTES system. Air is used as a heat transfer fluid (HTF) for the LHTES system. A ventilation system delivers fresh air to cool down the storage unit, normally during night-time to early morning, thereby solidifying the PCM. This process is called charging period. Thereafter, during discharging period, the hot air coming from internal heating loads is mixed with fraction of fresh air and then directed to pass over the centralized LHTES system resulting in a release of accumulation of stored cooling energy due to the change in phase of PCM thereby stabilizing the fluctuation of indoor air-temperature.

4.2. Indoor Temperatures

To analyze the performance of the storage system for one-day, the operational strategy should be followed along with associated assumptions as:

1-Relatively low air flow rates are allowed to pass over a canalized LHTES system during discharge period, normally from 6:00AM in the early morning until 19:00PM, seeking to flatten the fluctuation of inlet air temperatures within comfort temperature range from storage system outlet. To this end, fraction of fresh air is mixed with return air stream which is coming from the recirculation air inside the building to be delivered into the centralized LHTES system through an installation duct of the ventilation system. Mixed air is cooled down by the centralized LHTES system before being supplied to the building. However, if the outlet air-temperature from the centralized LHTES system is higher than the ambient air-temperature, fresh air is directed to the building without resorting to pass it into the centralized LHTES system.

These steps are performed in TRNSYS as following:

Air change function is scheduled using Type 14h to allow the air change per hour (ACH) of 5 vol/hr to supply into the building during the period of (19:00PM-6:00AM) and only allowed air change fraction of 2 vol/hr for the rest of the day. The indoor air is re-circulated and mixed with fraction of fresh air as performed in previous step in scheduled function as defined in prior. Fresh air-temperature is provided from Type9a for July month, in Montreal and re-circulated air-temperature is delivered from Type56.

The centralized LHTES Type is a function of time and temperature. This function is obtained after simulating a 3-D LHTES transient numerical model to solve heat transfer phase change problem of paraffin RT20 during July month. The Eq. (21) which is a second-order polynomial formula represents the outlet air-temperature of the centralized LHTES system. This formula is obtained after training ANN with data extracted from CFD simulation for the centralized LHTES system of 650mm length size.

$$Temp_{LHTES} = 2.7\times10^{-5} + 6.3\times10^{-3}\times Time - 4.1\times10^{-5}\times Temp - 2.3\times10^{-6}\times Time^2 - 0.03\times Temp^2 + 5.9\times10^{-3}\times Time \times Temp \quad (21)$$

where $Temp_{LHTES}$ is the outlet air-temperature of the centralized LHTES system, $Time$ is the simulation time (hr), and is called from Type9a as the ambient air-temperature is reading based on hourly changes according to weather data for Montreal.

Bypass ventilation control is applied to ensure suitable ventilation for the building. The temperature of mixed air which includes fresh ambient air and the LHTES's outlet air-temperature are linked to bypass check point. A lower air-temperature is chosen to be supplied into the building through the Type56 using a control functions. The control function has two conditions; first condition is allocated to check the air stream temperatures that are coming from the outside environment and the centralized LHTES system. Second condition is to check the temperatures of fresh air stream and re-circulated air stream. Thereafter, the control function is used to select the air stream which has a lower air-temperature to be supplied into the building.

2- At charging period, from 19:00PM until 6:00AM in the morning, higher air flow rates are preferable to solidify the PCM since the ambient temperatures are relatively low than melting point temperature of PCM. This cycle is periodically repeated.

Figure 5. shows the variation of the indoor air-temperature which is affected by the outlet ambient and the LHTES's outlet air-temperatures. During July month, it is obvious that the value of ambient air-temperature goes down in the middle of the week which enhances the night ventilation and therefore the LHTES system is almost completely charged.

However, the opportunity to take advantage of night ventilation decreases, when the ambient air-temperature increases, causing an increase of the indoor air-temperature. In general, the value of indoor air-temperature is relatively weighted the summation of the outlet ambient and LHTES' outlet air-temperatures as illustrated in Figure 6.

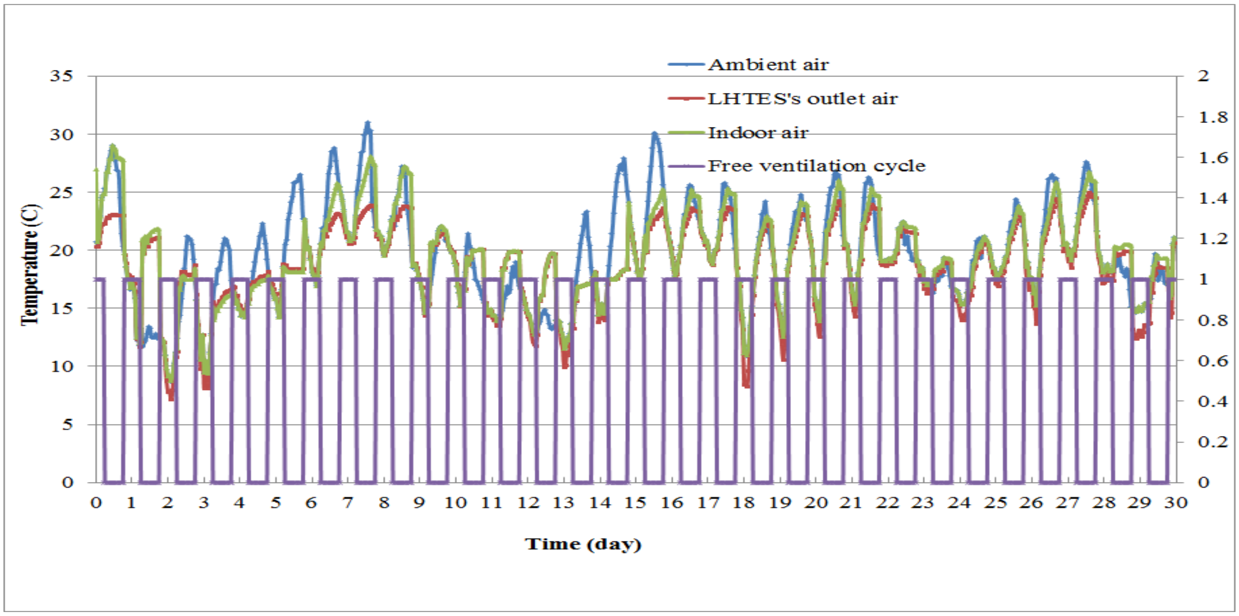

Figure 5. The Variation of Indoor Air-Temperature of The Building Model Integrating Into The LHTES System For Passive Space

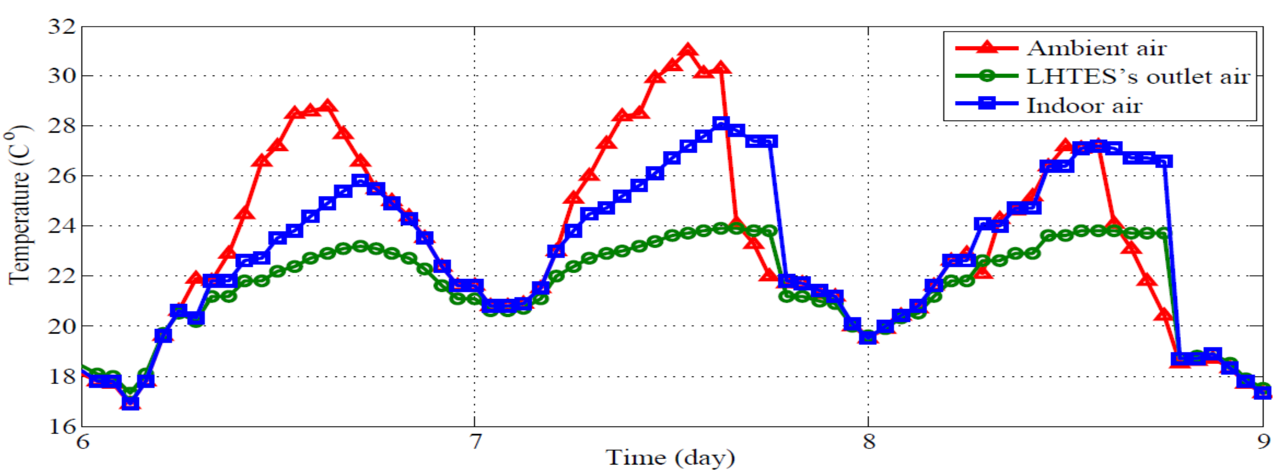

Figure 6. The Variation of Indoor Air-Temperature of The Building Model Integrating Into The LHTES System For (6-9) Days of July For Passive Space

Figure 7. shows different scenarios of indoor air-temperature using the LHTES system and night ventilation mode. No cooling auxiliary supply is provided during the selected period. To analyze the effect of night ventilation system with and without the centralized LHTES system, three days (6-9) of July are chosen from the summer season. The LHTES's response function in conjunction with night ventilation has a significant effect on reducing the variations of indoor air-temperature compared with only implementing night ventilation. This is attributed to the thermal storage effect of the centralized LHTES system in which the coldness of air stream is stored during night-time and then it is recovered to indoor air during day-time. The cooling effect of the centralized LHTES system lasts from 9:00 in morning to 17:00 in afternoon. This is due to the fact that PCM almost completely melts. Therefore, it suggests that the centralized LHTES system not only can stabilize the temperature swing but also improve the level of comfort inside the building. As can be seen from Figure 7, the indoor air-temperature raises due to the internal load when there is no a mechanical ventilation system to be applied, resulting in worming the space of the building model. However, an auxiliary cooling supply is needed to maintain the indoor air-temperature with the comfortable range below 28℃ because of high ACH during the daily operating of the building.

5. CONCLUSION

A validated 3-D centralized Latent Heat Thermal Energy Storage system (LHTES) transient numerical model is used to solve the conjugate phase change heat transfer and fluid flow problem using Computational Fluid Dynamic (CFD) commercial package, Fluent. The centralized LHTES system is filled with paraffin RT20 as a Phase Change Material (PCM) and is enhanced with fins embedded at the top and bottom of its surfaces. LHTES system is integrated with the mechanical ventilation system of low energy building to provide the required indoor thermal condition using free cooling. To analyze the LHTES thermal performance and its contribution to enhance energy performance inside a building, two operational strategies are applied. First, charging period strategy is applied from 19:00PM until 6:00AM in the morning. Higher air flow rates are preferable to solidify the PCM since the ambient air-temperature is relatively low than melting point temperature of PCM. The control strategy for a ventilated room is established to ensure that the internal air room temperature did not exceed 25℃. The National Climate Data and Information Archive in Canada weather data are used. The daily ambient air-temperature variations are recorded based on hourly changes. Second, discharge period is applied when relatively low air flow rates are allowed to pass over a canalized LHTES system from 6:00AM in the early morning until 19:00PM, thereby reducing the fluctuation of inlet ambient air-temperatures within comfort temperature range. Due to the fact that the computational time is significantly expensive, the simulations are performed separately for first days of each week through the month, in turn; the numerical database is used to train the Artificial Neural Network (ANN) method. Thereafter, the outlet LHTES's air-temperatures is extrapolated over the entire summer time-from the beginning of June to the end of August. The reduction of the indoor air-temperature is found in the range of 1.5-2.5℃.

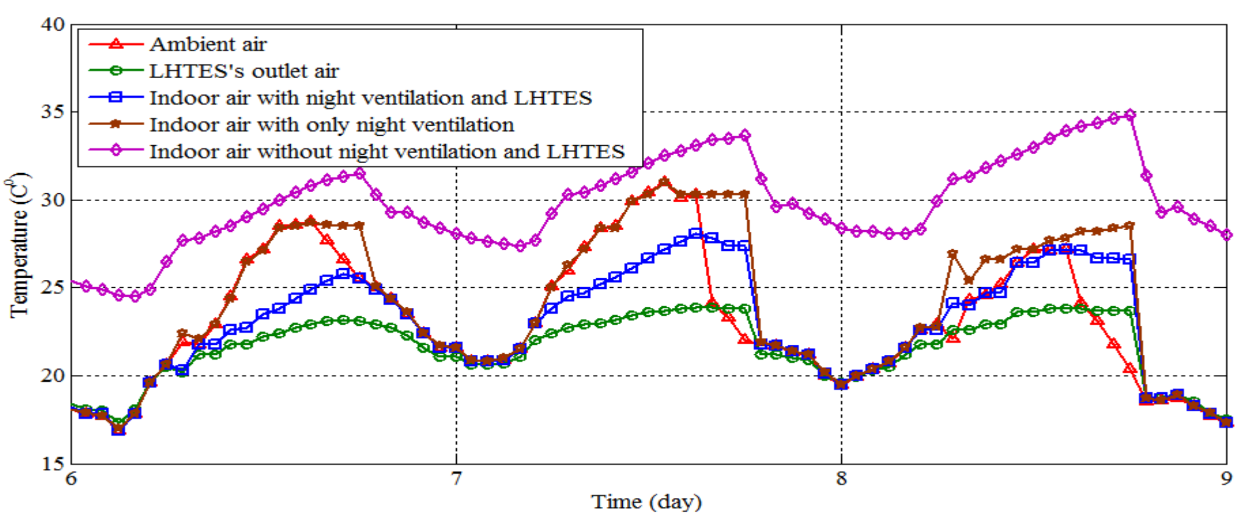

Figure 7. Indoor Air Temperature Histories With and Without LHTES System Combined With Night Ventilation For (6−9) Days of July

REFERENCES

A. El-Sawi, F. Haghighat and H. Akbari (2013). " Centralized latent heat thermal energy storage system: Model development and validation." Energy and Buildings, Energy and the Environment http://dx.doi.org/10.1016/j.enbuild.2013.05.027.

Agyenim, F., N. Hewitt, P. Eames and M. Smyth (2010). "A review of materials, heat transfer and phase change problem formulation for latent heat thermal energy storage systems (LHTESS)." Renewable and Sustainable Energy Reviews **14**(2): 615-628.

ANSYS FLUENT 12.0 User's Guide, R. A., Inc. 2009.

Arkar, C. and S. Medved (2007). "Free cooling of a building using PCM heat storage integrated into the ventilation system." Solar Energy **81**(9): 1078-1087.

Brent, A. D., V. R. Voller and K. J. Reid (1988). "Enthalpy-porosity technique for modeling convection-diffusion phase change: application to the melting of a pure metal." Numerical Heat Transfer **13**(3): 297-318.

Carman, P. C. (1937). "Fluid flow through granular beds." Trans. Inst. Chem. Engrs **15**: 150-156

Dincer, I., K. Ermis and A. Erek (2007). "Heat transfer analysis of phase change process in a finned-tube thermal energy storage system using artificial neural network." International Journal of Heat and Mass Transfer **50**(15-16): 3163-3175.

Farlow, S. J. (1984). Self-organizing methods in modeling: GMDH type algorithms, CRC.

Humphries, W. R. and E. I. Griggs (1977). "A design handbook for phase change thermal control and energy storage devices." NASA STI/Recon Technical Report N **78**: 15434.

Ivakhnenko, A. G. (1971). "Polynomial theory of complex systems." IEEE Transactions on Systems, Man and Cybernetics **SMC-1**(4): 364-378.

Parameshwaran, R., S. Kalaiselvam, S. Harikrishnan and A. Elayaperumal (2012). "Sustainable thermal energy storage technologies for buildings: A review." Renewable and Sustainable Energy Reviews **16**(5): 2394-2433.

Reid, R. C., J. M. Prausnitz and B. E. Poling (1987). "The properties of gases and liquids."

Soares, N., J. J. Costa, A. R. Gaspar and P. Santos (2013). "Review of passive PCM latent heat thermal energy storage systems towards buildings' energy efficiency." Energy and Buildings **59**: 82-103.

Stritih, U. and V. Butala (2010). "Experimental investigation of energy saving in buildings with PCM cold storage." International Journal of Refrigeration **33**(8): 1676-1683.

Voller, V. R., M. Cross and N. C. Markatos (1987). "An enthalpy method for convection/diffusion phase change." International Journal for Numerical Methods in Engineering **24**(1): 271-284.

Voller, V. R. and C. R. Swaminathan (1991). "General source-based method for solidification phase change." Numerical Heat Transfer, Part B (Fundamentals) **19**(2): 175-189.

Zhou, D., C. Y. Zhao and Y. Tian (2012). "Review on thermal energy storage with phase change materials (PCMs) in building applications." Applied Energy **92**: 593-605.